Transactions Letters

Low Complexity Pilot Assisted Carrier Frequency Offset Estimation for OFDMA Uplink Systems

Kilbom Lee, *Student Member, IEEE*, Sung-Hyun Moon, *Member, IEEE*, Sang-Rim Lee, *Student Member, IEEE* and Inkyu Lee, *Senior Member, IEEE*

***Abstract*—In this letter, we propose a low complexity pilot aided carrier frequency offset (CFO) estimation algorithm for orthogonal frequency division multiplexing access (OFDMA) uplink systems based on two consecutive received OFDMA symbols. Assuming that the channels and the CFOs are static over the two consecutive symbols, we express the second received OFDMA symbol in terms of the CFOs and the first OFDMA symbol. Based on this signal model, a new estimation algorithm which obtains the CFOs by minimizing the mean square distance between the received OFDMA symbol and its regenerated signal is provided. Also, we implement the proposed algorithm via fast Fourier transform (FFT) operations by utilizing the block matrix inversion lemma and the conjugate gradient method. Simulation results show that the proposed algorithm approaches the average Cramer Rao bound for moderate and high signal to noise ratio (SNR) regions. Moreover, the algorithm can be applied for any carrier assignment schemes with low complexity.**

***Index Terms*—CFO, estimation, synchronization, OFDMA.**

I. Introduction

ORTHOGONAL frequency division multiplexing access (OFDMA) is a promising transmission system due to its high spectrum efficiency and robustness to inter-symbol interference [1]. In the OFDMA, mobile users (MUs) can be simultaneously served by allocating a group of subcarriers according to a carrier assignment scheme (CAS), which includes a subband-based CAS (SCAS), an interleaved CAS (ICAS) and a generalized CAS (GCAS) [2]. However, the OFDMA is sensitive to carrier frequency offset (CFO) which arises from Doppler shifts or transceiver oscillator instabilities. The CFO results in severe inter-carrier interference (ICI) and multiple access interference (MAI) among subcarriers, which significantly degrade the bit error rate (BER) performance.

A CFO estimation problem can be classified into an acquisition stage and a tracking stage. In the acquisition stage, the CFO estimates are usually obtained at the beginning of each new frame by utilizing a training sequence which comprises symbols known to the base station (BS). There have been several papers devoted to the estimation of CFOs based on the training sequence for uplink OFDMA systems [3]–[5]. The main advantage of using the training sequence is that the BS can easily regenerate the received signal based on the estimated CFOs and channels [3]–[5].

In general, a pilot-aided algorithm is preferable in terms of spectral efficiency compared to a training sequence based algorithm. A gain in the spectral efficiency is more apparent when the acquisition step is needed frequently. However, it is difficult for a pilot-aided estimation algorithm to regenerate the received signal because the BS does not know all of the transmitted data. Therefore, it is more challenging to estimate the CFOs by using pilots for uplink OFDMA systems. For this reason, only a few works have been reported to solve the problem in uplink OFDMA systems [6], [7]. Recently, the authors in [6] and [7] provided a pilot-aided acquisition scheme and a tracking algorithm for uplink OFDMA systems, respectively, based on two consecutive OFDMA symbols which have a tile structure[1]. Also, those require several inverse operations of matrix whose size equals the number of subcarriers.

In this letter, we will develop a new low complexity pilot-aided algorithm for uplink OFDMA systems with the GCAS. Assuming that the channels and the CFOs of MUs are static over two consecutive OFDMA symbols, we represent the second OFDMA symbol as the signal which includes the CFOs and the first OFDMA symbol. By utilizing linear approximation presented in [3], we approximate this nonlinear model by a linear one in order to adopt a line search method. Thereby, a joint estimation algorithm is provided which obtains the CFOs and data by minimizing the mean square distance between the received second OFDMA symbol and its regenerated signal. Also, by using the block matrix inversion lemma and the conjugate gradient (CG) method in [8], we implement the proposed algorithm without computationally demanding inverse operations. Simulation results demonstrate that the proposed algorithm approaches the average Cramer Rao bound (CRB) in moderate and high signal to noise ratio

Manuscript received June 29, 2011; revised January 3, 2012; accepted April 8, 2012. The associate editor coordinating the review of this paper and approving it for publication was A. Ghrayeb.

This work was supported in part by the National Research Foundation of Korea (NRF) grant funded by the Korea government (MEST) (No. 2010-0017909), and in part by the Seoul R&BD program (WR080951).

K. Lee, S.-R. Lee, and I. Lee are with the School of Electrical Engineering, Korea University, Seoul, Korea (e-mail: {bachhi, sangrim78, inkyu}@korea.ac.kr).

S.-H. Moon is with the Electronics and Telecommunications Research Institute (ETRI), Daejeon, Korea (e-mail: sh.moon@etri.re.kr).

Digital Object Identifier 10.1109/TWC.2012.052512.111241

[1]A small group of adjacent subcarriers contains pilots and data symbols from one user [6].

(SNR) regions for any CAS.

Throughout this letter, normal letters represent scalar quantities, boldface lowercase letters indicate vectors, and boldface uppercase letters designate matrices. We use $(\cdot)^T$, $(\cdot)^\dagger$ and $\|\cdot\|$ for transpose, complex conjugate transpose and the 2-norm operation, respectively. In addition, $\Re\{c\}$ and $\Im\{c\}$ represent the real and imaginary components of c, respectively. The subscripts $[\cdot]_k$ and $[\cdot]_{i,j}$ designate the k-th element in a vector and the (i,j)-th entry in a matrix, respectively. $\mathbf{I}_l$ and $\mathbf{0}_{l\times n}$ denote an identity matrix of size $l\times l$ and a zero matrix of size $l\times n$, respectively. Also, diag$\{\mathbf{x}\}$ stands for a diagonal matrix whose diagonal elements are defined by $\mathbf{x}$.

II. Signal Model

In this letter, we consider uplink OFDMA systems with N subcarriers, N_g cyclic prefix length and K MUs. Let us define the channel impulse response vector $\mathbf{h}_k$ as $\mathbf{h}_k = [h_{0,k}\ h_{1,k}\ \cdots\ h_{L-1,k}]^T$ where $h_{i,k}$ has an independent and identically distributed (i.i.d.) complex Gaussian distribution and L stands for the channel length. We suppose that the channel is static over two consecutive OFDMA symbols, which is reasonable in practical situations [6] [7]. The set $\mathcal{C}_k$ consists of the subcarrier indices of the k-th MU, and we assume that $\mathcal{C}_k \cap \mathcal{C}_l = \phi$ for $k \neq l$ and $\cup_{k=1}^{K}\mathcal{C}_k = \{0,\cdots,N-1\}$. The CFO of the k-th MU is defined as ϵ_k which is normalized by the subcarrier spacing and assumed to be static over two consecutive OFDMA symbols. We denote $\mathbf{F} = [\mathbf{f}_0\ \mathbf{f}_1\cdots\mathbf{f}_{N-1}]$ as the $N\times N$ discrete Fourier transform (DFT) matrix with $\mathbf{f}_i = \frac{1}{\sqrt{N}}[1\ e^{\frac{-j2\pi i}{N}}\cdots\ e^{\frac{-j2\pi i(N-1)}{N}}]^T$, and define $\mathbf{F}_L = [\mathbf{f}_0\ \mathbf{f}_1\cdots\mathbf{f}_{L-1}]$. Then, the diagonal channel matrix $\mathbf{H}_k$ is given as $\mathbf{H}_k = \sqrt{N}\text{diag}\{\mathbf{F}_L\mathbf{h}_k\} = \text{diag}\{H_{0,k}, H_{1,k},\cdots,H_{N-1,k}\}$ where $H_{i,k}$ is the channel gain of the i-th subcarrier for the k-th MU. Moreover, the l-th transmitted signal of the k-th MU can be obtained as $\mathbf{x}_{k,l} = [X^k_{0,l}\ \cdots\ X^k_{N-1,l}]^T$ where $X^k_{i,l} = 0$ for $i \notin \mathcal{C}_k$.

Then, the received consecutive OFDMA symbols are represented in the frequency domain as

$$\mathbf{r}_l = \mathbf{F}\sum_{k=1}^{K}\mathbf{\Gamma}_l(\epsilon_k)\mathbf{F}^\dagger\mathbf{H}_k\mathbf{x}_{k,l} + \mathbf{w}_l \quad \text{for } l = 1,2 \tag{1}$$

where $\mathbf{\Gamma}_1(\epsilon_k) = \text{diag}\{1,\ \exp\left(\frac{j2\pi\epsilon_k}{N}\right),\cdots,\exp\left(\frac{j2\pi(N-1)\epsilon_k}{N}\right)\}$ equals a diagonal matrix whose diagonal entry stands for the phase shift of the corresponding received signal sample, we define $\mathbf{\Gamma}_2(\epsilon_k) = e^{j2\pi\epsilon_k N_t/N}\mathbf{\Gamma}_1(\epsilon_k)$ with $N_t = N + N_g$, and $\mathbf{w}_l = [w_{0,l}\ w_{1,l}\cdots\ w_{N-1,l}]^T$ indicates the complex additive white Gaussian noise (AWGN) vector with zero mean and covariance matrix $\sigma_w^2\mathbf{I}_N$.

Let us define a diagonal matrix $\mathbf{\Psi}_k$ of size N where $[\mathbf{\Psi}_k]_{i,i} = 1$ for $i \in \mathcal{C}_k$ and $[\mathbf{\Psi}_k]_{i,i} = 0$ otherwise. Then, we denote the composite transmitted data for MUs as $\bar{\mathbf{x}}_l = \sum_{k=1}^{K}\mathbf{\Psi}_k\mathbf{x}_{k,l} = [\bar{X}_{0,l}\ \bar{X}_{1,l}\ \cdots\ \bar{X}_{N-1,l}]^T$ where $\bar{X}_{i,l} = X^k_{i,l}$ for $i \in \mathcal{C}_k$. Similar to $\bar{\mathbf{x}}_l$, the composite channel frequency response is defined as $\bar{\mathbf{H}} = \sum_{k=1}^{K}\mathbf{\Psi}_k\mathbf{H}_k = \text{diag}\{\bar{H}_0,\ \bar{H}_1,\ \cdots,\ \bar{H}_{N-1}\}$ where $\bar{H}_i = H_{i,k}$ for $i \in \mathcal{C}_k$.

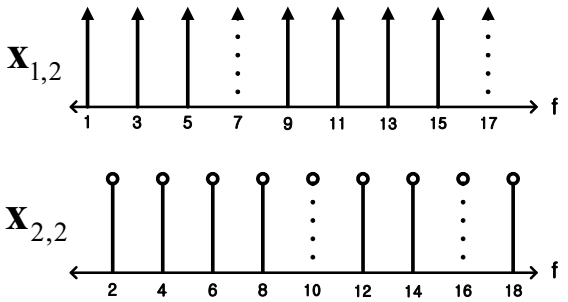

Fig. 1. Transmitted OFDM symbols of each MU at the second time slot in the frequency domain

Then, the expression in (1) can be rewritten as

$$\begin{aligned}\mathbf{r}_l &= \left(\sum_{k=1}^{K}\mathbf{C}_l(\epsilon_k)\mathbf{\Psi}_k\right)\bar{\mathbf{H}}\bar{\mathbf{x}}_l + \mathbf{w}_l \quad \text{for } l = 1,2\\ &= \mathbf{Q}_l\bar{\mathbf{H}}\bar{\mathbf{x}}_l + \mathbf{w}_l\end{aligned} \tag{2}$$

where $\mathbf{C}_l(\epsilon_k) = \mathbf{F}\mathbf{\Gamma}_l(\epsilon_k)\mathbf{F}^\dagger$ is a circulant matrix and $\mathbf{Q}_l = \sum_{k=1}^{K}\mathbf{C}_l(\epsilon_k)\mathbf{\Psi}_k$ stands for the interference matrix caused by CFOs. Note that $\mathbf{Q}_l$ becomes an identity matrix if all CFOs are zero. By applying the zero-forcing filter based on the estimated CFOs, the compensated received signal can be obtained as $\mathbf{g}_l = {\mathbf{Q}_l}^{-1}\mathbf{r}_l$. If the estimated CFOs are so accurate that interference of subcarriers are sufficiently suppressed, $\bar{\mathbf{x}}_l$ can be detected from $\mathbf{g}_l$ by using an one-tap equalizer.

III. Proposed Pilot-aided Estimation Algorithms

In this section, we derive a new CFO estimation algorithm which utilizes the two consecutive OFDMA symbols based on a line search method. To obtain the initial CFOs, a simple method is also provided.

A. New representation of the second received OFDMA symbol

Here, we describe some preliminary definitions and mathematical results related to $\mathbf{r}_1$ and $\mathbf{r}_2$. Let us define $\mathbf{b}$ and $\mathbf{B}$ as $\mathbf{b} = [b_0\ \cdots\ b_{N-1}]$ with $b_m = \bar{X}_{m,2}/\bar{X}_{m,1}$ and $\mathbf{B} = \text{diag}\{\mathbf{b}\}$, respectively, where b_m equals zero if the m-th subcarrier is null. By using $\mathbf{r}_1$, $\mathbf{B}$ and the CFOs, the second received OFDMA symbol $\mathbf{r}_2$ can be rewritten as

$$\begin{aligned}\mathbf{r}_2 &= \mathbf{Q}_2\bar{\mathbf{H}}\bar{\mathbf{x}}_2 + \mathbf{w}_2 = \mathbf{Q}_2\bar{\mathbf{H}}\mathbf{B}\bar{\mathbf{x}}_1 + \mathbf{w}_2\\ &= \mathbf{Q}_2\mathbf{B}\mathbf{Q}_1^{-1}\mathbf{Q}_1\bar{\mathbf{H}}\bar{\mathbf{x}}_1 + \mathbf{w}_2 = \mathbf{Q}_2\mathbf{B}\mathbf{Q}_1^{-1}(\mathbf{r}_1 - \mathbf{w}_1) + \mathbf{w}_2\\ &= \mathbf{Q}_2\mathbf{B}\mathbf{Q}_1^{-1}\mathbf{r}_1 + \mathbf{n}\end{aligned} \tag{3}$$

where $\mathbf{n}$ is expressed as $\mathbf{n} = \mathbf{w}_2 - \mathbf{Q}_2\mathbf{B}\mathbf{Q}_1^{-1}\mathbf{w}_1$.

In (3), an unknown parameter set is given by $\{\epsilon_1,\cdots,\epsilon_K,\ \ b_0,\cdots,b_{N-1}\}$. Since the number of the unknown elements is $N+K$ and the size of equation (3) is N, at least K elements in $\mathbf{b}$ should be known to the BS in advance. For this reason, we assume that $\bar{X}_{m,2}$ is equal to $\bar{X}_{m,1}$ (i.e. $b_m = 1$) for certain subcarriers where the number of those is equal to or greater than K. Based on this knowledge, we will jointly estimate the CFOs and the remaining unknown part of $\mathbf{b}$. With some abuse of terminology, the known and unknown elements in $\mathbf{b}$ are referred to as pilots and differential data, respectively. Then,

we denote $\mathbf{p} = [1 \ \cdots \ 1]^T$ and $\mathcal{C}_p$ as the vector which consists of N_p pilots of all MUs with $N_p \geq K$ and the set which contains the indices of pilots, respectively. Similarly, we define $\mathbf{d} = [d_1 \ \cdots \ d_{N_d}]^T$ and $\mathcal{C}_d$ as the vector which comprises N_d unknown differential data of all MUs with $N_d = N - N_p$ and the corresponding set, respectively.

Fig. 1 illustrates an example of $\mathbf{x}_{1,2}$ and $\mathbf{x}_{2,2}$ in the frequency domain where $\mathcal{C}_1$ and $\mathcal{C}_2$ are defined as $\{1, 3, \cdots, 17\}$ and $\{2, 4, \cdots, 18\}$, respectively. Moreover, $\mathcal{C}_p$ and $\mathcal{C}_d$ are defined as $\{7, 10, 16, 17\}$ and $\{\mathcal{C}_1 \cup \mathcal{C}_2\} \setminus \mathcal{C}_p$, respectively[2]. Then, $\bar{X}_{m,2}$, denoted by a dotted line, is equal to $\bar{X}_{m,1}$ for $m \in \mathcal{C}_p$, which leads to a reduction of the data rate as $\frac{2N-N_p}{2N}$ in two OFDMA symbols[3].

By using $\mathcal{C}_p$ and $\mathcal{C}_d$, we represent a diagonal matrix $\tilde{\mathbf{\Phi}}_p$ where $[\tilde{\mathbf{\Phi}}_p]_{i,i} = 1$ for $i \in \mathcal{C}_p$ and $[\tilde{\mathbf{\Phi}}_p]_{i,i} = 0$ otherwise. Extracting the columns whose indices are contained in $\mathcal{C}_p$ from $\tilde{\mathbf{\Phi}}_p$ yields $\mathbf{\Phi}_p$ of size $N \times N_p$. Similarly, $\mathbf{\Phi}_d$ of size $N \times N_d$ can be defined with $\mathcal{C}_d$. Then, it can be checked that we have $\mathbf{\Phi}_p^T\mathbf{\Phi}_p = \mathbf{I}_{N_p}$, $\mathbf{\Phi}_d^T\mathbf{\Phi}_d = \mathbf{I}_{N_d}$ and $\mathbf{\Phi}_p^T\mathbf{\Phi}_d = \mathbf{0}_{N_p \times N_d}$. Thereby, the vector $\mathbf{b}$ is given by

$$\mathbf{b} = \mathbf{\Phi}_p\mathbf{p} + \mathbf{\Phi}_d\mathbf{d} \tag{4}$$

where $\mathbf{p}$ and $\mathbf{d}$ can be obtained as $\mathbf{\Phi}_p^T\mathbf{b}$ and $\mathbf{\Phi}_d^T\mathbf{b}$, respectively.

By utilizing (4), the received signal $\mathbf{r}_2$ in (3) can be rewritten as

$$\begin{aligned} \mathbf{r}_2 &= \mathbf{Q}_2\tilde{\mathbf{R}}_1\mathbf{b} + \mathbf{n} \\ &= \mathbf{Q}_2\tilde{\mathbf{R}}_1\mathbf{\Phi}_p\mathbf{p} + \mathbf{Q}_2\tilde{\mathbf{R}}_1\mathbf{\Phi}_d\mathbf{d} + \mathbf{n} \end{aligned} \tag{5}$$

where $\tilde{\mathbf{R}}_1 = \mathrm{diag}\{\mathbf{Q}_1^{-1}\mathbf{r}_1\}$. Note that $\mathbf{n}$ has a correlated covariance matrix $\mathbf{C}_n = \sigma_w^2\big(\mathbf{I}_N + \mathbb{E}[\mathbf{Q}_2\mathbf{B}\mathbf{Q}_1^{-1}(\mathbf{Q}_1^{-1})^\dagger\mathbf{B}^\dagger\mathbf{Q}_2^\dagger]\big)$, and $\mathbf{Q}_1$ and $\mathbf{Q}_2$ are unknown. Therefore, it is impossible to consider exact value of $\mathbf{C}_n$. To facilitate the analysis, we assume that all MUs' CFOs are adequately small so as to justify an uncorrelated approximation as[4] [7]

$$\mathbf{C}_n \simeq 2\sigma_w^2\mathbf{I}_N. \tag{6}$$

B. Proposed estimation algorithm

Now, we develop an one-shot algorithm to jointly estimate the CFOs and the unknown part of $\mathbf{b}$ from the signal model in (5) based on a line search method. Let us define the unknown parameter vector and the initial estimated corresponding vector as $\mathbf{u} = [\boldsymbol{\xi}^T \ \mathbf{d}^T]^T$ with $\boldsymbol{\xi} = [\epsilon_1 \ \cdots \ \epsilon_K]^T$ and $\hat{\mathbf{u}}^{(0)} = [(\hat{\boldsymbol{\xi}}^{(0)})^T \ (\hat{\mathbf{d}}^{(0)})^T]^T$ with $\hat{\boldsymbol{\xi}}^{(0)} = [\hat{\epsilon}_1^{(0)} \ \cdots \ \hat{\epsilon}_K^{(0)}]^T$ and $\hat{\mathbf{d}}^{(0)} = [\hat{d}_1^{(0)} \ \cdots \ \hat{d}_{N_d}^{(0)}]^T$, respectively. From our new expression for $\mathbf{r}_2$ in (3), we can regenerate $\mathbf{r}_2^{(0)}$ by using $\mathbf{r}_1$ and $\hat{\mathbf{u}}^{(0)}$ as

$$\mathbf{r}_2^{(0)} = \mathbf{Q}_2^{(0)}\mathbf{B}^{(0)}(\mathbf{Q}_1^{(0)})^{-1}\mathbf{r}_1$$

where $\mathbf{B}^{(0)}$, $\mathbf{Q}_1^{(0)}$ and $\mathbf{Q}_2^{(0)}$ are obtained from the initial estimated vector $\hat{\mathbf{u}}^{(0)}$.

[2]In this case, $\mathbf{b}$ is given by $[d_1 \ \cdots \ d_6 \ 1 \ d_7 \ d_8 \ 1 \ d_9 \ \cdots \ d_{13} \ 1 \ 1 \ d_{14}]^T$.

[3]For our proposed algorithm, it is not necessary to know the transmitted data $\bar{X}_{m,1}$ for $m \in \mathcal{C}_p$.

[4]If all CFOs are zero and the constant-magnitude constellation such as 4-QAM is employed, we have $\mathbf{C}_n = 2\sigma_w^2\mathbf{I}_N$.

Note that $\mathbf{r}_2$ in (5) is a nonlinear function of $\mathbf{u}$ due to the CFOs. By applying the first-order Taylor series expansion in [3], we can approximate $\mathbf{r}_2$ as a linear function of $\mathbf{u}$

$$\mathbf{r}_2 \ \approx \ \mathbf{r}_2^{(0)} + \mathbf{G}(\mathbf{u} - \hat{\mathbf{u}}^{(0)}) + \mathbf{n} \tag{7}$$

where the gradient matrix $\mathbf{G}$ of size $N \times (N_d + K)$ is defined as

$$\begin{aligned} \mathbf{G} &\triangleq \left[\frac{\partial\mathbf{r}_2}{\partial\epsilon_1} \ \cdots \ \frac{\partial\mathbf{r}_2}{\partial\epsilon_K} \ \frac{\partial\mathbf{r}_2}{\partial\mathbf{d}}\right]_{\mathbf{u}=\hat{\mathbf{u}}^{(0)}} \\ &= \big[\mathbf{t}(\hat{\epsilon}_1^{(0)}) \ \cdots \ \mathbf{t}(\hat{\epsilon}_K^{(0)}) \ \mathbf{G}_2\big]. \end{aligned} \tag{8}$$

Here, $\mathbf{t}(\hat{\epsilon}_k^{(0)})$ and $\mathbf{G}_2$ are derived, respectively, as

$$\begin{aligned} \mathbf{t}(\hat{\epsilon}_k^{(0)}) &\triangleq \left.\frac{\partial\mathbf{r}_2}{\partial\epsilon_k}\right|_{\mathbf{u}=\mathbf{u}^{(0)}} \\ &= \frac{j2\pi}{N}\Big\{\mathbf{F}(\mathbf{M} + N_t\mathbf{I})\mathbf{\Gamma}_2(\hat{\epsilon}_k^{(0)})\mathbf{F}^\dagger\mathbf{\Psi}_k\mathbf{B}^{(0)}\mathbf{g}_1^{(0)} \\ &\quad - \mathbf{Q}_2^{(0)}\mathbf{B}^{(0)}(\mathbf{Q}_1^{(0)})^{-1}\mathbf{F}\mathbf{M}\mathbf{\Gamma}_1(\hat{\epsilon}_k^{(0)})\mathbf{F}^\dagger\mathbf{\Psi}_k\mathbf{g}_1^{(0)}\Big\} \\ \mathbf{G}_2 &\triangleq \left.\frac{\partial\mathbf{r}_2}{\partial\mathbf{d}}\right|_{\mathbf{u}=\mathbf{u}^{(0)}} = \mathbf{Q}_2^{(0)}\tilde{\mathbf{R}}_1^{(0)}\mathbf{\Phi}_d \end{aligned}$$

where we have $\mathbf{M} = \mathrm{diag}\{0, \ \cdots, N-1\}$, $\mathbf{g}_1^{(0)} = (\mathbf{Q}_1^{(0)})^{-1}\mathbf{r}_1$ and $\tilde{\mathbf{R}}_1^{(0)} = \mathrm{diag}\{(\mathbf{Q}_1^{(0)})^{-1}\mathbf{r}_1\}$. Note that the accuracy of the approximation in (7) depends on the initial estimated vector $\hat{\mathbf{u}}^{(0)}$.

Now, we define a trial vector of $\mathbf{u}$ as $\tilde{\mathbf{u}}^{(1)} = [(\tilde{\boldsymbol{\xi}}^{(1)})^T \ (\tilde{\mathbf{d}}^{(1)})^T]^T$. Based on (7) and $\tilde{\mathbf{u}}^{(1)}$, the regenerated signal $\tilde{\mathbf{r}}_2^{(1)}$ is obtained as

$$\tilde{\mathbf{r}}_2^{(1)} \ = \ \mathbf{r}_2^{(0)} + \mathbf{G}(\tilde{\mathbf{u}}^{(1)} - \hat{\mathbf{u}}^{(0)}). \tag{9}$$

By minimizing the mean square distance between $\mathbf{r}_2$ in (7) and $\tilde{\mathbf{r}}_2^{(1)}$ in (9), we find the new estimated vector $\hat{\mathbf{u}}^{(1)}$ which is formulated as

$$\begin{aligned} \hat{\mathbf{u}}^{(1)} &= \arg\min_{\tilde{\mathbf{u}}^{(1)}} \big\{\mathbb{E}\|\mathbf{r}_2 - \tilde{\mathbf{r}}_2^{(1)}\|^2\big\} \\ &\approx \arg\min_{\tilde{\mathbf{u}}^{(1)}} \big\{\mathbb{E}\|\mathbf{G}(\mathbf{u} - \tilde{\mathbf{u}}^{(1)}) + \mathbf{n}\|^2\big\}. \end{aligned} \tag{10}$$

Then, the problem (10) can be solved by a line search method as [3] [4]

$$\hat{\mathbf{u}}^{(1)} = \hat{\mathbf{u}}^{(0)} + \big(\mathbf{G}^\dagger\mathbf{G}\big)^{-1}\mathbf{G}^\dagger(\mathbf{r}_2 - \mathbf{r}_2^{(0)}). \tag{11}$$

Since the performance of the solution in (11) depends on $\hat{\mathbf{u}}^{(0)}$, we will address an initial estimation method for $\hat{\mathbf{u}}^{(0)}$ in the following subsection.

Now, we derive the CRB of the CFO for the joint estimation of CFOs and the unknown differential data $\mathbf{d}$. Based on (3) and (6), the likelihood function of $\mathbf{r}_2$ conditioned on $\mathbf{u}$ and $\mathbf{r}_1$ is written by

$$f(\mathbf{r}_2|\mathbf{u}, \mathbf{r}_1) = \frac{1}{(2\pi\sigma_w^2)^N}\exp\Big(-\frac{1}{2\sigma_w^2}\|\mathbf{r}_2 - \mathbf{Q}_2\mathbf{B}\mathbf{Q}_1^{-1}\mathbf{r}_1\|^2\Big).$$

By utilizing the results in [9], the CRB for the CFO of the k-th MU is obtained as

$$\mathrm{CRB}(\epsilon_k) = \sigma_w^2\left[\Big(\Re\big\{\mathbf{Z}^\dagger\big(\mathbf{I} - \mathbf{P}(\mathbf{P}^\dagger\mathbf{P})^{-1}\mathbf{P}^\dagger\big)\mathbf{Z}\big\}\Big)^{-1}\right]_{k,k} \tag{12}$$

where $\mathbf{Z} = [\mathbf{t}(\epsilon_1) \ \cdots \ \mathbf{t}(\epsilon_K)]$ and $\mathbf{P} = \mathbf{Q}_2\tilde{\mathbf{R}}_1\mathbf{\Phi}_d$.

C. Initialization of unknown parameters

To ensure the accuracy of the algorithm in (11), we describe a method to estimate the initial CFOs and the unknown differential data $\hat{\mathbf{u}}^{(0)} = [(\hat{\boldsymbol{\xi}}^{(0)})^T \ (\hat{\mathbf{d}}^{(0)})^T]^T$ with pilots. We assume that $\mathcal{C}_k \cap \mathcal{C}_p$ is not an empty set for $k = 1, \cdots, K$, which indicates that each MU has at least one pilot. To expand (2), let us define the m-th element of $\mathbf{r}_l$ as $R_{m,l}$. Then, we can obtain the initial estimate of ϵ_k as

$$\begin{aligned}\hat{\epsilon}_k^{(0)} &= \frac{N}{2\pi N_t} \arg\left\{ \sum_{m \in \mathcal{C}_k \cap \mathcal{C}_p} R_{m,1}^* R_{m,2} \right\} \qquad (13)\\ &\approx \frac{N}{2\pi N_t} \arg\left\{ e^{j2\pi\epsilon_k N_t/N} \sum_{m \in \mathcal{C}_k \cap \mathcal{C}_p} |\Upsilon(\epsilon_k)|^2 |\bar{H}_m \bar{X}_{m,2}|^2 \right\}\end{aligned}$$

where $\Upsilon(\epsilon) \triangleq \frac{1}{N} e^{j\pi\epsilon\frac{N-1}{N}} \frac{\sin(\pi\epsilon)}{\sin(\pi\epsilon/N)}$, and the approximation comes from ignoring the noise, the ICI and the MAI. Note that this initial CFO estimator is similar to the conventional algorithm in [10].

Let us define $\mathbf{g}_2^{(0)}$ as $\mathbf{g}_2^{(0)} = \left(\mathbf{Q}_2^{(0)}\right)^{-1}\mathbf{r}_2$. Here, $\mathbf{g}_1^{(0)}$ and $\mathbf{g}_2^{(0)}$ are expected to have lower ICI and MAI than $\mathbf{r}_1$ and $\mathbf{r}_2$, respectively. Therefore, more accurate initial estimates of ϵ_k can be obtained by repeating the step in (13) based on $\mathbf{g}_1^{(0)}$ and $\mathbf{g}_2^{(0)}$. Then, $\mathbf{g}_1^{(0)}$ and $\mathbf{g}_2^{(0)}$ are recalculated by using the second initial CFO estimates.

On the other hand, the initial estimate $\hat{\mathbf{d}}^{(0)}$ is computed as

$$\hat{\mathbf{d}}^{(0)} = (\mathrm{diag}\{\boldsymbol{\Phi}_d^T \mathbf{g}_1^{(0)}\})^{-1} \boldsymbol{\Phi}_d^T \mathbf{g}_2^{(0)}. \qquad (14)$$

Then, we obtain $\hat{\mathbf{u}}^{(0)} = [(\hat{\boldsymbol{\xi}}^{(0)})^T \ (\hat{\mathbf{d}}^{(0)})^T]^T$.

IV. Low Complexity Implementations and Algorithm

A. CG-based implementations

In this subsection, we present a low complexity implementation of our proposed algorithm with the CG method. From $(\mathbf{G}^\dagger\mathbf{G})^{-1}$ in (11) and $\mathbf{g}_l^{(0)} = \left(\mathbf{Q}_l^{(0)}\right)^{-1}\mathbf{r}_l$ in (14), we see that most of the computational complexity comes from matrix inversions. To avoid the inverse operations, we employ the CG method which is an iterative algorithm for solving linear equations with a positive-definite matrix[5] [8].

First, $\mathbf{g}_l^{(0)} = \left(\mathbf{Q}_l^{(0)}\right)^{-1}\mathbf{r}_l$ in (14) can be rewritten as a linear equation

$$\left(\mathbf{Q}_l^{(0)}\right)^\dagger \mathbf{Q}_l^{(0)} \mathbf{g}_l^{(0)} = \left(\mathbf{Q}_l^{(0)}\right)^\dagger \mathbf{r}_l \quad \text{for} \ \ l = 1, 2. \qquad (15)$$

Here, we check that $\left(\mathbf{Q}_l^{(0)}\right)^\dagger \mathbf{Q}_l^{(0)}$ is a positive definite matrix and $\mathbf{Q}_l^{(0)} = \mathbf{F}\sum_{k=1}^K \boldsymbol{\Gamma}_l(\epsilon_k^{(0)})\mathbf{F}^\dagger\boldsymbol{\Psi}_k$ comprises the DFT matrices. In this case, the CG method can solve a linear equation such as (15) via fast Fourier transform (FFT) operations [11]. Then, the computational complexity for obtaining $\mathbf{g}_l^{(0)}$ is reduced from $O(N^3)$ to $O(I_{cg}KN\log N)$ with I_{cg} denoting the iteration number of the CG method. Moreover, the authors in [11] show that a solution to the problem (15) can be found within a few iterations[6] which are much smaller than N. Especially, for the ICAS system, the iteration number I_{cg} for an exact solution is at most K.

On the contrary, for $(\mathbf{G}^\dagger\mathbf{G})^{-1}$ in (11), the CG method cannot solve this inverse problem by the FFT operations, and thus the computational complexity becomes $O(I_{cg}(N_d+K)N)$. In addition, it requires as many iterations as $I_{cg} = N_d + K$ to obtain a solution unlike equation (15). For this reason, we transform equation (11) to facilitate an FFT-based CG method. We first denote $\left[\mathbf{t}(\hat{\epsilon}_1^{(0)}) \ \cdots \ \mathbf{t}(\hat{\epsilon}_K^{(0)})\right]$ in (8) as $\mathbf{G}_1$ with $\mathbf{G} = \left[\mathbf{G}_1\mathbf{G}_2\right]$. By applying the block matrix inversion lemma to $(\mathbf{G}^\dagger\mathbf{G})^{-1}$ in (11), the new estimate $\hat{\boldsymbol{\xi}}^{(1)}$ is extracted as [12]

$$\hat{\boldsymbol{\xi}}^{(1)} = \hat{\boldsymbol{\xi}}^{(0)} + \mathbf{T}^{-1}\left(\mathbf{G}_1^\dagger - \mathbf{A}^\dagger\mathbf{G}_2^\dagger\right)(\mathbf{r}_2 - \hat{\mathbf{r}}_2^{(0)}) \qquad (16)$$

where $\mathbf{A} = (\mathbf{G}_2^\dagger\mathbf{G}_2)^{-1}\mathbf{G}_2^\dagger\mathbf{G}_1$ and $\mathbf{T} = \mathbf{G}_1^\dagger\mathbf{G}_1 - \mathbf{A}^\dagger\mathbf{G}_2^\dagger\mathbf{G}_1$ whose sizes equal $N_d \times K$ and $K \times K$, respectively. Here, we see that the computation of $\mathbf{A}$ requires high computational complexity $O(N_d^3 + NN_d^2)$ due to $(\mathbf{G}_2^\dagger\mathbf{G}_2)^{-1}$. Therefore, we rewrite $\mathbf{A}$ as

$$\mathbf{G}_2^\dagger\mathbf{G}_2\mathbf{A} = \mathbf{Y}$$

where $\mathbf{Y} \triangleq \mathbf{G}_2^\dagger\mathbf{G}_1$. Defining the l-th column of $\mathbf{A}$ and $\mathbf{Y}$ as $\mathbf{a}_l$ and $\mathbf{y}_l$, respectively, $\mathbf{a}_l$ can be represented as a linear equation

$$\begin{aligned}\mathbf{G}_2^\dagger\mathbf{G}_2\mathbf{a}_l &= \boldsymbol{\Phi}_d^\dagger(\tilde{\mathbf{R}}_1^{(0)})^\dagger\left((\mathbf{Q}_2^{(0)})^\dagger\mathbf{Q}_2^{(0)}\right)\tilde{\mathbf{R}}_1^{(0)}\boldsymbol{\Phi}_d\mathbf{a}_l\\ &= \mathbf{y}_l \quad \text{for} \ \ l = 1, \cdots, K \qquad (17)\end{aligned}$$

where note that $\tilde{\mathbf{R}}_1^{(0)} = \mathrm{diag}\{\mathbf{g}_1^{(0)}\}$ is a diagonal matrix. Similar to (15), the above equation can be solved by the CG method implemented by the FFT operations. Also, the new estimate $\hat{\mathbf{d}}^{(1)}$ is obtained from (14) based on the estimated $\hat{\boldsymbol{\xi}}^{(1)}$. By applying the CG method to the problems (15) and (17), the proposed algorithm can be implemented without computationally expensive inverse operations. Also, simulation results show that the proposed scheme implemented with the CG method approaches the CRB for moderate and high SNR regions.

B. Low complexity CFO estimator

From equations (8), (15) and (17), it can be checked that the algorithm needs $2K+4$ CG operations. In this subsection, we present a low complexity CFO estimator based on the CFO estimator (16) to reduce the number of the CG operations.

Let us define the residual CFOs in $\left(\mathbf{Q}_1^{(0)}\right)^{-1}\mathbf{r}_1 = \mathbf{g}_1^{(0)}$ and $\left(\mathbf{Q}_2^{(0)}\right)^{-1}\mathbf{r}_2 = \mathbf{g}_2^{(0)}$ as $\Delta\epsilon_k^{(1)}$. In addition, we assume that $\Delta\epsilon_k^{(1)} = \epsilon_k - \hat{\epsilon}_k^{(0)}, \ k = 1, \cdots, K$. Then, we can replace the regenerated signal $\hat{\mathbf{r}}_2^{(0)}$ and the observation signal $\mathbf{r}_2$ in (16) with the compensated signals $\mathbf{B}^{(0)}\mathbf{g}_1^{(0)}$ and $\mathbf{g}_2^{(0)}$, respectively. In this case, the initial CFO estimates used for $\mathbf{A}, \mathbf{T}, \mathbf{G}_1$ and $\mathbf{G}_2$ in (16) are reset to zero, because the initial CFO estimates (i.e. $\hat{\epsilon}_k^{(0)}$) are compensated from $\mathbf{r}_1$ and $\mathbf{r}_2$ in advance. Hence, the CFO estimator (16) can be simplified to

$$\hat{\boldsymbol{\xi}}^{(1)} = \hat{\boldsymbol{\xi}}^{(0)} + \tilde{\mathbf{T}}^{-1}\left(\tilde{\mathbf{G}}_1^\dagger - \tilde{\mathbf{A}}^\dagger\tilde{\mathbf{G}}_2^\dagger\right)(\mathbf{g}_2^{(0)} - \mathbf{B}^{(0)}\mathbf{g}_1^{(0)}) \qquad (18)$$

[5]For a positive definite matrix with size N, the CG is guaranteed to converge and can find an exact solution within N iterations [8].

[6]This is due to the fact that all eigenvalues of the matrix $\mathbf{Q}_l^\dagger\mathbf{Q}_l$ are clustered in a very narrow range [11].

TABLE I
COMPUTATION LOADS OF ALL ALGORITHMS

	Number of Complex Multiplications
LS	$(2K+4)I_{cg}KN\log N + \frac{4+K}{2}N\log N$
LLS	$4I_{cg}KN\log N + 2KN\log N + 4N_dK + \frac{3}{2}K^2N_d$
AHE	$\frac{4}{3}N^3 + 6N_p$
GS	$\frac{4}{3}N^3 + 6GNN_p$

where $\tilde{\mathbf{A}} = (\tilde{\mathbf{G}}_2^\dagger\tilde{\mathbf{G}}_2)^{-1}\tilde{\mathbf{G}}_2^\dagger\tilde{\mathbf{G}}_1$ and $\tilde{\mathbf{T}} = \tilde{\mathbf{G}}_1^\dagger\tilde{\mathbf{G}}_1 - \tilde{\mathbf{A}}^\dagger\tilde{\mathbf{G}}_2^\dagger\tilde{\mathbf{G}}_1$. Here, $\tilde{\mathbf{G}}_1 = \left[\tilde{\mathbf{t}}_1 \ \cdots \ \tilde{\mathbf{t}}_K\right]$ and $\tilde{\mathbf{G}}_2$ are given, respectively, by

$$\tilde{\mathbf{t}}_k = \frac{j2\pi}{N}\left\{\mathbf{F}(\mathbf{M}+N_t\mathbf{I})\mathbf{F}^\dagger\mathbf{\Psi}_k\mathbf{B}^{(0)}\mathbf{g}_1^{(0)} - \mathbf{B}^{(0)}\mathbf{F}\mathbf{M}\mathbf{F}^\dagger\mathbf{\Psi}_k\mathbf{g}_1^{(0)}\right\}$$

$$\tilde{\mathbf{G}}_2 = \mathrm{diag}\{\mathbf{g}_1^{(0)}\}\mathbf{\Phi}_d$$

where we check that $\tilde{\mathbf{G}}_2^\dagger\tilde{\mathbf{G}}_2$ becomes a diagonal matrix and $\tilde{\mathbf{t}}_k$ does not involve matrix inversion. As a result, the required number of the CG operations is reduced from $2K+4$ to 4.

Note that the CFO estimator (18) produces the CFO estimates as $\hat{\epsilon}_k^{(1)} = \hat{\epsilon}_k^{(0)} + \Delta\hat{\epsilon}_k^{(1)}$. However, the estimate $\hat{\epsilon}_k^{(1)}$ cannot converge to ϵ_k even though $\Delta\hat{\epsilon}_k^{(1)} = \Delta\epsilon_k^{(1)}$. This is due to the fact that the residual CFO $\Delta\epsilon_k^{(1)}$ is not exactly[7] identical to $\epsilon_k - \hat{\epsilon}_k^{(0)}$, which means that the CFO estimator (18) is biased. As a result, we expect that the low-complexity CFO estimator (18) produces degraded performance compared to the CFO estimator (16), which will be shown in the simulation section.

V. SIMULATION RESULTS

In this section, we compare the computational complexity and the mean square error (MSE) performance of our proposed algorithms with those of other conventional algorithms in OFDMA uplink systems with 128 subcarriers, $N_g = 16$ and $K = 4$. We assume a 5-tap Rayleigh fading exponential decaying channel and perform $1,000$ simulation runs. In addition, $\{\epsilon_1, \cdots, \epsilon_K\}$ are independently chosen from a uniform distribution within a range $[-0.3, 0.3]$. For simple simulations, each MU is randomly assigned to $P = N/K$ subcarriers. Also, the number of pilots and unknown differential data of each MU is set to N_p/K and N_d/K ($N = N_p + N_d$), respectively. In addition, we employ differential quadrature phase shift keying (DQPSK). The iteration number I_{cg} of the CG method is set to 16.

For simple notation, we call the proposed line search based algorithm in (16) and the low complexity one in (18) as LS and LLS, respectively. Also, the grid search algorithm [6] and the ad hoc CFO estimator [7] are referred to as GS and AHE, respectively.

The initial estimates of the proposed algorithms are obtained from the initial stages in (13) and (14). For the GS, the number of grid points G is chosen to be 601 over the range of $[-0.3, 0.3]$ to achieve the precision of 10^{-3}, and the iteration number is set to 3. Also, the iteration number of the AHE is set to 3. Table I and Fig. 2 illustrate the number of complex multiplications of all algorithms for different numbers of subcarriers with $K = 4$ and the tile size $Z = 4$. It can be seen that the LLS has the smallest computational complexity which is almost the same as that of the 4 CG operations. This is due to the fact that the computational complexity of the LLS mainly depends on the CG operation. In contrast, the LS shows relatively high computational complexity, while having the same slope with respect to N. For the GS, its computational complexity is the highest due to the grid search and inverse operations.

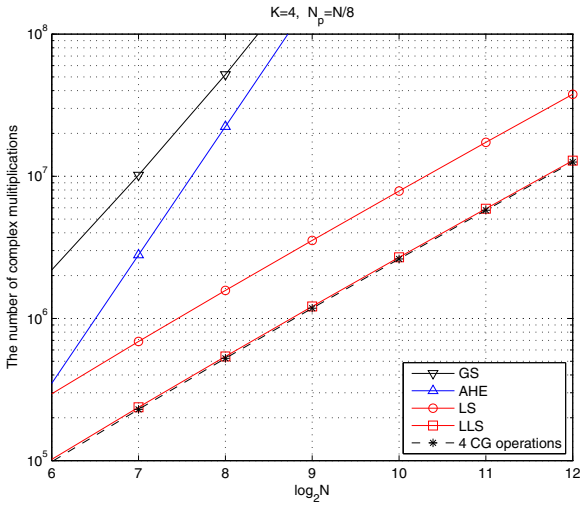

Fig. 2. Comparison of computational complexity with $K = 4$

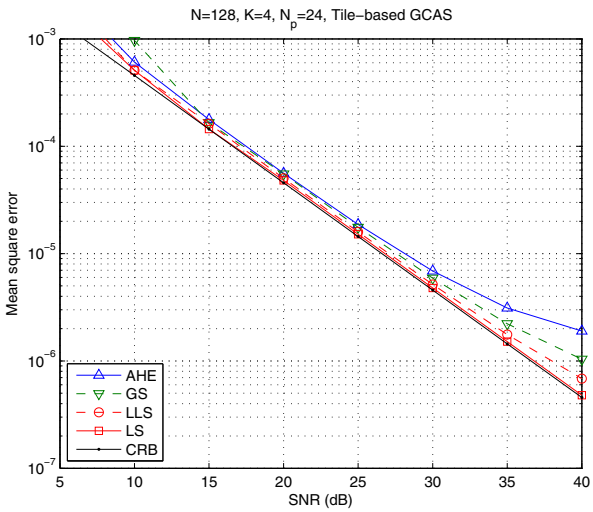

Fig. 3. MSE performance of CFO estimators with different algorithms

Fig. 3 compares the MSE performance of the proposed algorithms with those of the conventional algorithms. Here, we employ the tile-based GCAS with $Z = 4$. The average CRB is obtained by averaging the CRB in (12) over multiple simulation runs with different random CFOs and channel gains. It can be seen that all algorithms yield higher MSE at low SNR. This can be explained by the fact that the algorithms produce large CFO errors at low SNR. In the SNR higher than 10 dB, the LS approaches the average CRB. As expected, the LLS yields slightly degraded performance in moderate and

[7]The residual CFO $\Delta\epsilon_k^{(1)}$ is generally not equal to $\epsilon_k - \hat{\epsilon}_k^{(0)}$ because $\mathbf{Q}_l^{-1}(\hat{\epsilon}_k^{(0)})\mathbf{Q}_l(\epsilon_k) \neq \mathbf{Q}_l(\epsilon_k - \hat{\epsilon}_k^{(0)})$ where $\mathbf{Q}_l(\epsilon_k)$ denotes $\mathbf{Q}_l$ matrix with $\{\epsilon_1, \cdots, \epsilon_K\}$. In contrast, for $K = 1$, we have $\mathbf{Q}_l^{-1}(\hat{\epsilon}_1^{(0)})\mathbf{Q}_l(\epsilon_1) = \mathbf{F}\mathbf{\Gamma}_l(-\hat{\epsilon}_1^{(0)})\mathbf{F}^\dagger\mathbf{F}\mathbf{\Gamma}_l(\epsilon_1)\mathbf{F}^\dagger = \mathbf{Q}_l(\epsilon_1 - \hat{\epsilon}_1^{(0)}) = \mathbf{Q}_l(\Delta\epsilon_1^{(1)})$, which indicates that both estimators (16) and (18) produce the same estimate $\hat{\epsilon}_1^{(1)}$.

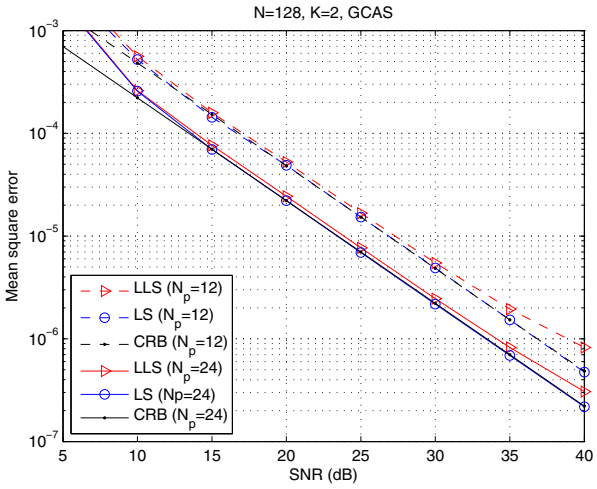

Fig. 4. MSE performance of proposed algorithms with different numbers of pilots

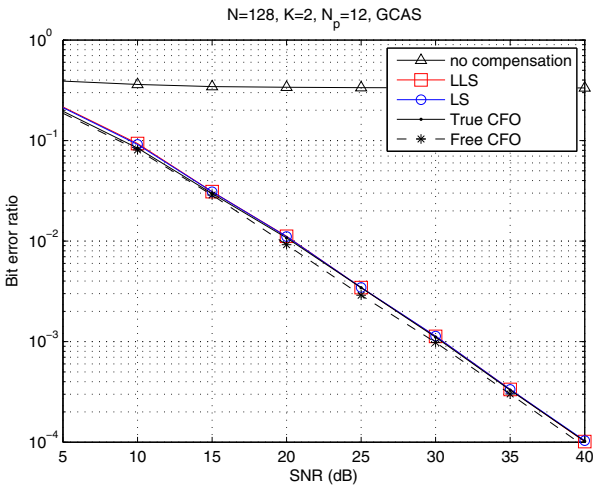

Fig. 5. BER performance of proposed algorithms with $N_p = 12$

high SNR regions with substantially reduced computational complexity, and the performance gap slowly increases as SNR increases. Compared to the LLS, the GS and the AHE produce higher performance loss in moderate and high SNR regions, and the performance gap are about 2.5 dB and 5 dB at the SNR of 40 dB, respectively.

Fig. 4 illustrates the MSE performance of our proposed algorithms according to the number of pilots. Contrary to the previous simulation, the GCAS with $Z = 1$ and $K = 2$ is employed. We see that our proposed algorithms with $N_p = 24$ achieve a 3 dB performance gain over those with $N_p = 12$. It is clear that our proposed algorithms can effectively obtain a good trade-off between the MSE performance and the spectral efficiency for the GCAS. Furthermore, we see that the performance gap between the LS and the LLS decreases as the number of pilots increases.

Fig. 5 compares the BER performance of the LS with that of the LLS for $N_p = 12$. In the case of true CFOs, the BS determines the unknown differential data $\mathbf{d}$ from $\mathbf{g}_l = \mathbf{Q}_l^{-1}\mathbf{r}_l$ where $\mathbf{Q}_l^{-1}$ is given by the true CFOs. The BER performance of the LS is almost identical to that of the true CFO case, while an 1 dB loss is observed compared to the case of no CFOs. Especially, the LLS yields the same BER performance as the LS over all SNR regions. As a result, the LLS can provide higher spectral efficiency with a negligible BER performance loss and significantly reduced computational complexity.

VI. Conclusions

In this letter, we have proposed a pilot-aided joint estimation method for CFOs and the unknown differential data for OFDMA uplink systems. Based on the first received OFDMA symbol, we represent the second OFDMA symbol as the signal which includes the CFOs, the pilots and the unknown differential data. Then, by approximating this nonlinear model with a linear function, we have proposed a new joint estimation algorithm motivated by the line search method. Also, the proposed algorithm can be implemented via FFT operations through the CG method. We confirm from simulation results that the proposed algorithm aided by the initial estimation method can approach the average CRB in moderate and high SNR regions with low complexity even for small pilots. As a result, our proposed algorithms provide a good trade-off between the MSE performance and the spectral efficiency with low complexity for general carrier assignment schemes.

References

[1] "IEEE standard for local and metropolitan area networks, Part 16: Air Interface for Fixed and Mobile Broadband Wireless Access Systems Amendment 2: Physical and Medium Access Control Layers for Combined Fixed and Mobile operation in Licensed Bands," IEEE Std. 802.16e, Feb. 2006.

[2] C. Y. Wong, R. S. Cheng, K. B. Letaief, and R. D. Murch, "Multicarrier OFDM with adaptive subcarrier, bit, and power allocation," *IEEE J. Sel. Areas Commun.*, vol. 17, pp. 479–483, Oct. 1999.

[3] Y. Na and H. Minn, "Line search based iterative joint estimation of channels and frequency offsets for uplink OFDMA systems," *IEEE Trans. Wireless Commun.*, vol. 6, pp. 4374–4382, Dec. 2007.

[4] X. N. Zeng, A. Ghrayeb, and D. Mao, "CFO estimation for uplink OFDM systems: an application of the variable projection method," *IEEE Trans. Wireless Commun.*, vol. 8, pp. 2306–2311, May 2009.

[5] K. Lee, S.-H. Moon, and I. Lee, "Low-complexity leakage-based carrier frequency offset estimation techniques for OFDMA uplink systems," in *Proc. 2010 IEEE GLOBECOM*, pp. 1–5.

[6] P. Sun and L. Zhang, "Low complexity pilot aided frequency synchronization for OFDMA uplink transmission," *IEEE Trans. Wireless Commun.*, vol. 8, pp. 3758–3769, July 2009.

[7] P. Sun, M. Michele, and L. Zhang, "Carrier frequency offset tracking in the IEEE 802.16e OFDMA uplink," *IEEE Trans. Wireless Commun.*, vol. 9, pp. 3613–3619, Dec. 2010.

[8] J. R. Shewchuk, *An Introduction to the Conjugate-Gradient Method without the Agonizing Pain*. Carnegie Mellon University, School of Computer Science, 1994.

[9] O. Besson and P. Stoica, "On parameter estimation of MIMO flat-fading channels with frequency offsets," *IEEE Trans. Signal Process.*, vol. 51, pp. 602–613, Mar. 2003.

[10] L. Sanguinetti and M. Morelli, "A low-complexity scheme for frequency estimation in uplink OFDMA systems," *IEEE Trans. Wireless Commun.*, vol. 9, pp. 2430–2437, Aug. 2010.

[11] K. Lee and I. Lee, "CFO compensation for uplink OFDMA systems with conjugated gradient," in *Proc. 2011 IEEE ICC*.

[12] G. A. F. Seber and C. J. Wild, *Nonlinear Regression*. Wiley, 1989.